



Supplement of

Cloud-scale modelling of the impact of deep convection on the fate of oceanic bromoform in the troposphere: a case study over the west coast of Borneo

Paul D. Hamer et al.

Correspondence to: Paul D. Hamer (paul.hamer@nilu.no)

The copyright of individual parts of the supplement might differ from the article licence.

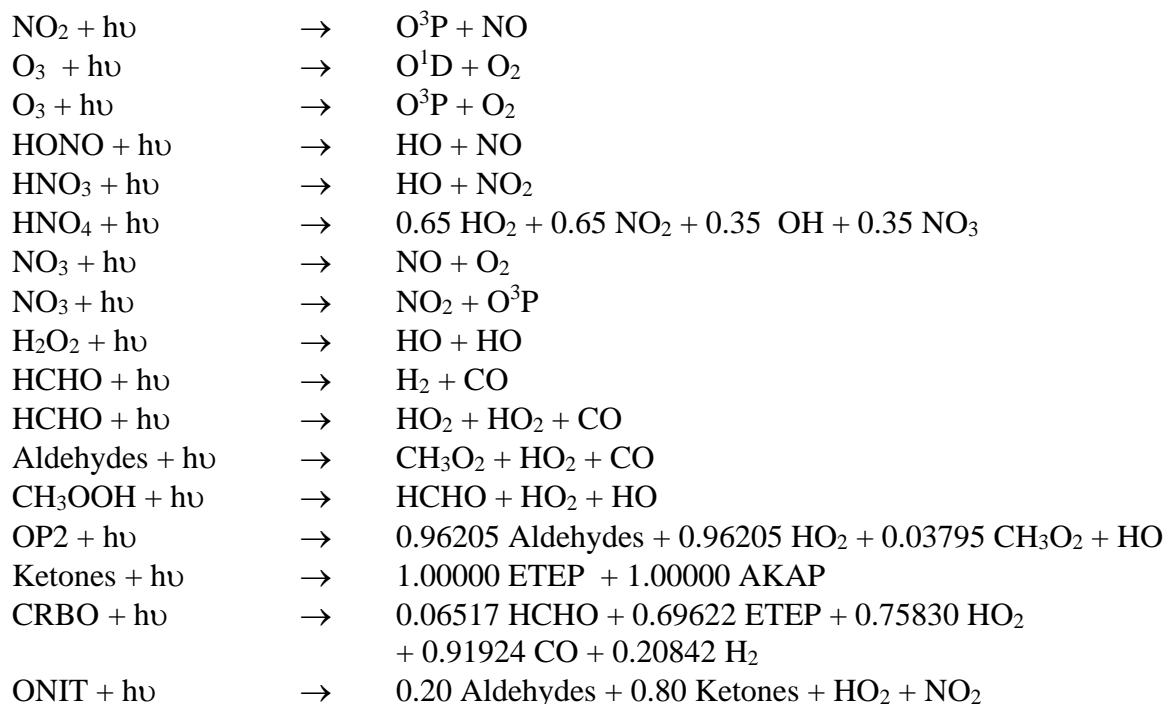
S1. RELASH Chemical Mechanism

We present the list of the chemical reactions in the RELASH mechanism. The RELASH mechanism is derived from the **ReLACS** scheme developed by Crassier et al., 2000, and we added halogen chemistry consistent with that developed by Hossaini et al., 2010 and Kryzstofiak et al., 2012 for **SHIVA**. All of the reaction rates associated with the ReLACS scheme are described in Stockwell et al., 1997 in table 2. The subsequent modifications to the NMHC chemistry reactions rates to move from RACM to ReLACS are described by Crassier et al., 2000 and listed in table 3. All of the halogen and VSLs gas phase chemical reaction rates unique to RELASH are described by Kryzstofiak et al., 2012 in table 4 of that article. Finally, the reaction rates for the aqueous phase halogen chemistry listed as unique to RELASH is described in detail within Marécal et al., 2012. Where appropriate specific details for the location of the detailed description are given.

We categorise all of the reactions according to whether they are photolysis, gas phase, or aqueous phase reactions.

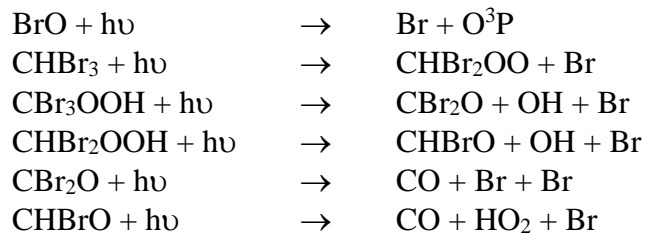
Photolysis

ReLACS



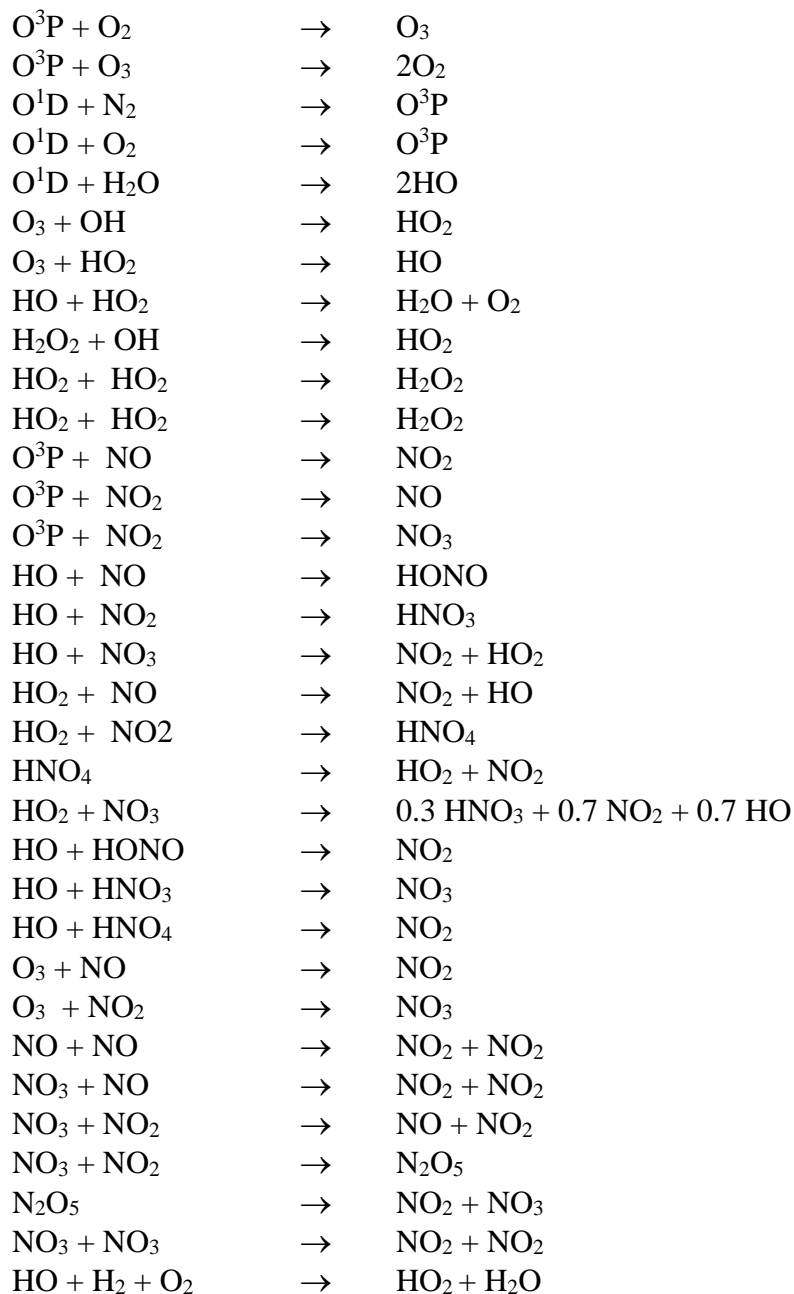
Unique to RELASH





Gas Phase

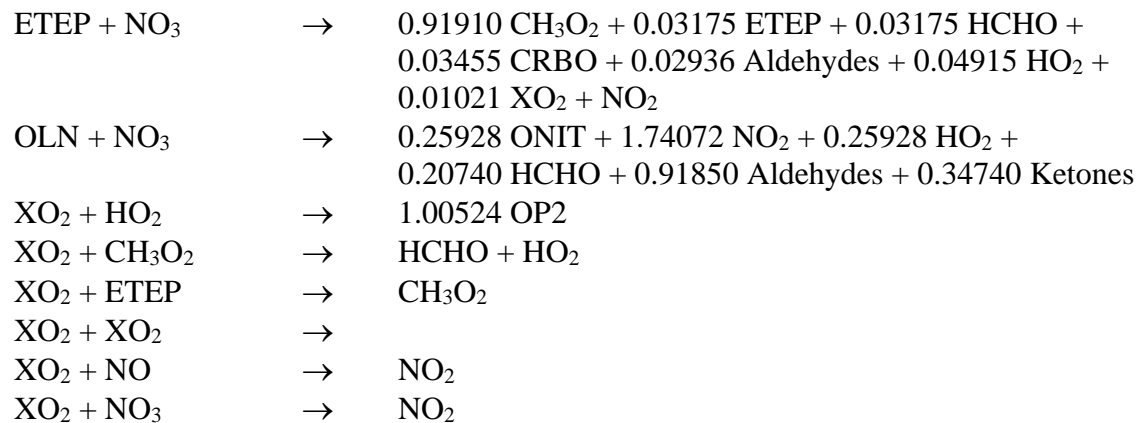
ReLACS



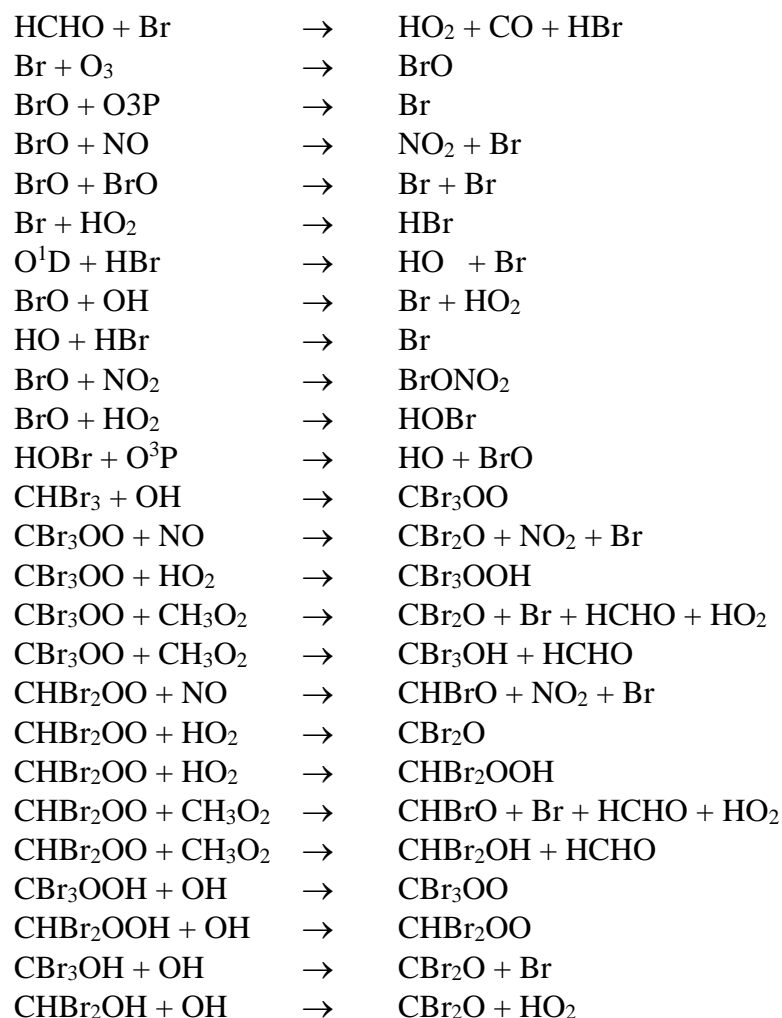
HO + SO ₂	→	SULF + HO ₂
CO + OH	→	HO ₂ + CO ₂
Biogenics + O ³ P	→	0.91868 Alkenes + 0.05 HCHO + 0.02 OH + 0.01 CO + 0.13255 CRBO + 0.28 HO ₂ + 0.15 XO ₂
CRBO + O ³ P	→	Aldehydes
CH ₄ + OH	→	CH ₃ O ₂
C ₂ H ₆ + OH	→	AKAP
Alkanes + OH	→	0.87811 AKAP + 0.12793 HO ₂ + 0.08173 Aldehydes + 0.03498 Ketones + 0.00835 CRBO + 0.00140 HCHO + 0.00878 ORA1 + .000878 CO + 0.000878 HO
Alkenes + OH	→	1.02529 AKEP + 0.00000 Bio Peroxys
Biogenics + OH	→	1.00000 Biogenic Peroxys
Aro + OH	→	0.93968 ADD + 0.10318 XO ₂ + 0.10318 HO ₂ + 0.00276 PHO
HCHO + OH	→	HO ₂ + CO
Aldehydes + OH	→	1.00000 ETEP
Ketones + OH	→	1.00000 ETEP
CRBO + OH	→	0.51419 ETEP + 0.16919 CRBO + 1.01732 CO + 0.51208 HO ₂ + 0.00000 HCHO + 0.06253 Aldehydes + 0.00853 Ketones + 0.10162 XO ₂ + 0.75196 H ₂ O
CH ₃ OOH + OH	→	0.65 CH ₃ O ₂ + 0.35 HCHO + 0.35 HO
OP2 + OH	→	0.40341 AKAP + 0.05413 ETEP + 0.07335 Aldehydes + 0.37591 Ketones + 0.09333 XO ₂ + 0.02915 HO ₂ + 0.02915 HCHO + 0.44925 HO
PAN + OH	→	0.57839 HCHO + 0.21863 CRBO + 0.71893 NO ₃ + 0.28107 PAN + 0.28107 HO ₂ + XO ₂ + 0.29733 H ₂ O
ONIT + OH	→	1.00000 AKAP + NO ₂
HCHO + NO ₃	→	HO ₂ + HNO ₃ + CO
Aldehydes + NO ₃	→	1.00000 ETEP + HNO ₃
CRBO + NO ₃	→	0.91567 HNO ₃ + 0.38881 ETEP + 0.10530 CRBO + 0.05265 Aldehydes + 0.00632 Ketones + 0.10530 NO ₂ + 0.10530 XO ₂ + 0.63217 HO ₂ + 1.33723 CO + 0.00000 OLN
Aro + NO ₃	→	HNO ₃ + PHO
Alkenes + NO ₃	→	0.00000 CRBO + 0.93768 OLN
Biogenics + NO ₃	→	0.91741 CRBO + 1.00000 OLN
PAN + NO ₃	→	0.60 ONIT + 0.60 NO ₃ + 0.40 PAN + 0.40 HCHO + 0.40 NO ₂ + XO ₂
Alkenes + O ₃	→	0.48290 HCHO + 0.51468 Aldehydes + 0.07377 Ketones + 0.00000 CRBO + 0.35120 CO + 0.15343 ORA1 + 0.08143 ORA2 + 0.23451 HO ₂ + 0.39435 OH +

		0.05705 ETEP + 0.03196 C ₂ H ₆ + 0.00000 Alkenes + 0.04300 CH ₄ + 0.13966 CH ₃ O ₂ + 0.09815 AKAP + 0.01833 H ₂ O ₂ + 0.00000 XO ₂ + 0.05409 H ₂ + 0.00000 O ³ P
Biogenics + O ₃	→	0.90000 HCHO + 0.00000 Aldehydes + 0.00000 Ketones + 0.39754 CRBO + 0.36000 CO + 0.37388 Alkenes + 0.00000 AKAP + 0.17000 ETEP + 0.03000 CH ₃ O ₂ + 0.15000 ORA1 + 0.00000 ORA2 + 0.28000 OH + 0.30000 HO ₂ + 0.00100 H ₂ O ₂ + 0.05000 H ₂ + 0.13000 XO ₂ + 0.09000 O ³ P
CRBO + O ₃	→	0.00000 HCHO + 1.07583 CRBO + 0.15692 Aldehydes + 0.10788 ORA1 + 0.20595 ORA2 + 0.27460 ETEP + 0.10149 OP2 + 0.64728 CO + 0.28441 HO ₂ + 0.20595 OH + 0.00000 H ₂
PAN + O ₃	→	0.70 HCHO + 0.30 PAN + 0.70 NO ₂ + 0.13 CO + 0.04 H ₂ + 0.11 ORA1 + 0.08 HO ₂ + 0.036 OH + 0.70 ETEP
PHO + NO ₂	→	0.10670 Aro + ONIT
PHO + HO ₂	→	1.06698 Aro
ADD + NO ₂	→	Aro + HONO
ADD	→	0.98 Aro Peroxys + 0.02 Aro + 0.02 HO ₂
ADD + O ₃	→	Aro + HO
ETEPA + NO ₂	→	1.00000 PAN
PAN	→	1.00000 ETEP + NO ₂
CH ₃ O ₂ + NO	→	HCHO + HO ₂ + NO ₂
AKAP + NO	→	0.33144 Aldehydes + 0.03002 HCHO + 0.54531 Ketones + 0.03407 CRBO + 0.74265 HO ₂ + 0.09016 CH ₃ O ₂ + 0.08187 AKAP + 0.13007 XO ₂ + 0.08459 ONIT + 0.91541 NO ₂
AKEP + NO	→	1.39870 HCHO + 0.42125 Aldehydes + 0.05220 Ketones + HO ₂ + NO ₂
Bio Peroxys+ NO	→	0.45463 CRBO + 0.60600 HCHO + 0.00000 Aldehydes + 0.00000 Ketones + 0.37815 Alkenes + 0.84700 HO ₂ + 0.84700 NO ₂ + 0.15300 ONIT
Aro Peroxys + NO	→	0.95115 NO ₂ + 0.95115 HO ₂ + 2.06993 CRBO + 0.04885 ONIT
ETEPA + NO	→	0.78134 CH ₃ O ₂ + 0.09532 ETEP + 0.05848 HCHO + 0.07368 Aldehydes + 0.08670 CRBO + 0.12334 HO ₂ + 0.02563 XO ₂ + NO ₂
OLN + NO	→	0.18401 ONIT + 1.81599 NO ₂ + 0.18401 HO ₂ + 0.23419 HCHO + 1.01182 Aldehydes + 0.37862 Ketones
CH ₃ O ₂ + HO ₂	→	CH ₃ OOH
AKAP + HO ₂	→	1.00524 OP2
AKEP + HO ₂	→	1.00524 OP2
Bio Peroxys+ HO ₂	→	1.00524 OP2

Aro Peroxys + HO ₂	→	1.00524 OP2
ETEP + HO ₂	→	0.80904 OP2 + 0.17307 ORA2 + 0.17307 O ₃
OLN + HO ₂	→	ONIT
CH ₃ O ₂ + CH ₃ O ₂	→	1.33 HCHO + 0.66 HO ₂
AKAP + CH ₃ O ₂	→	0.80556 HCHO + 0.98383 HO ₂ + 0.56070 Aldehydes + 0.09673 Ketones + 0.01390 CH ₃ O ₂ + 0.07976 CRBO + 0.13370 XO ₂ + 0.00385 AKAP
AKEP + CH ₃ O ₂	→	1.42894 HCHO + 0.46413 Aldehydes + 0.03814 Ketones + HO ₂
Bio Peroxys + CH ₃ O ₂	→	0.56064 CRBO + 0.48074 Alkenes + 1.00000 HO ₂ + 1.09000 HCHO + 0.00000 Aldehydes + 0.00000 Ketones
Aro Peroxys + CH ₃ O ₂	→	HCHO + 1.02767 HO ₂ + 1.99461 CRBO
ETEP + CH ₃ O ₂	→	0.95723 HCHO + 0.82998 HO ₂ + 0.56031 CH ₃ O ₂ + 0.13684 ORA2 + 0.05954 ETEP + 0.15387 CRBO + 0.08295 Aldehydes + 0.02212 XO ₂
OLN + CH ₃ O ₂	→	0.88625 HCHO + 0.67560 HO ₂ + 0.67560 ONIT + 0.41524 Aldehydes + 0.09667 Ketones + 0.32440 NO ₂
AKAP + ETEP	→	0.71461 Aldehydes + 0.48079 HO ₂ + 0.51480 CH ₃ O ₂ + 0.49810 ORA2 + 0.18819 Ketones + 0.07600 HCHO + 0.00828 AKAP + 0.11306 XO ₂ + 0.06954 CRBO
AKEP + ETEP	→	0.68192 HCHO + 0.68374 Aldehydes + 0.50078 HO ₂ + 0.50078 CH ₃ O ₂ + 0.49922 ORA2 + 0.06579 Ketones
Bio Peroxys + ETEP	→	0.78591 CRBO + 0.24463 Alkenes + 0.50600 HO ₂ + 0.49400 ORA2 + 0.34000 HCHO + 0.50600 CH ₃ O ₂ + 0.00000 Aldehydes + 0.00000 Ketones
Aro Peroxys + ETEP	→	CH ₃ O ₂ + HO ₂ + 1.99455 CRBO
ETEP + ETEP	→	1.66702 CH ₃ O ₂ + 0.05821 ETEP + 0.03432 HCHO + 0.10777 CRBO + 0.06969 Aldehydes + 0.02190 Ketones + 0.07566 HO ₂ + 0.01593 XO ₂ + 0.09955 ORA2
OLN + ETEP	→	0.66562 ONIT + 0.51037 CH ₃ O ₂ + 0.48963 ORA2 + 0.17599 HO ₂ + 0.13414 HCHO + 0.42122 Aldehydes + 0.10822 Ketones + 0.00000 NO ₂
OLN + OLN	→	2.00 ONIT + HO ₂
OLN + OLN	→	.353 HCHO + .925 Aldehydes + .217 Ketones + 0.500 HO ₂ + .750 NO ₂ + 1.250 ONIT
CH ₃ O ₂ + NO ₃	→	HCHO + HO ₂ + NO ₂
AKAP + NO ₃	→	0.33743 Aldehydes + 0.81290 HO ₂ + 0.03142 HCHO + 0.62978 Ketones + 0.03531 CRBO + 0.09731 CH ₃ O ₂ + 0.08994 AKAP + 0.16271 XO ₂ + NO ₂
AKEP + NO ₃	→	1.40909 HCHO + 0.43039 Aldehydes + 0.02051 Ketones + HO ₂ + NO ₂
Bio Peroxys + NO ₃	→	0.61160 CRBO + 0.42729 Alkenes + 0.68600 HCHO + 0.00000 Aldehydes + 0.00000 Ketones + HO ₂ + NO ₂
Aro Peroxys + NO ₃	→	2.81904 CRBO + HO ₂ + NO ₂



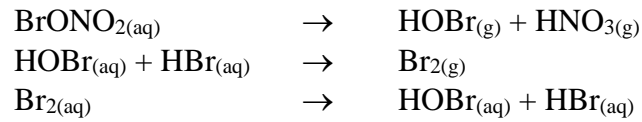
Unique to RELASH



Aqueous Phase

Unique to RELASH

Described in Section 2.2, pages 6076-6077, Marécal et al., 2012



OP2 = C₂ and higher organic peroxides

ORA2 = C₂ and higher organic acids

ONIT = Organic nitrate

ETEP = Peroxy radicals from ethane

XO₂ = Species accounting for additional NO to NO₂ conversions

CRBO = Glyoxal

AKAP = Peroxy radicals formed from ALKA

ADD = Aromatic-OH adduct

AKEP = Peroxy radicals formed from alkenes

S2. How the estimates of $[X]_{\text{BL}}$, $[X]_{\text{UTconv}}$, and $[X]_{\text{UTnoconv}}$ are determined from observations and the model

Here are the details on how we calculated the simulated and observed mixing ratios presented in Table 3. Following Krysztofiak et al. (2018), the mean mixing ratio estimates based on Falcon measurements for the

$[X]_{UTconv}$ and $[X]_{UTnoconv}$ (~11- 13 km altitude range) were split according to humidity data and webcam images corresponding to cloudy or cloud-free conditions, respectively. $[X]_{BL}$ are data gathered during the flight ascent/descent from/to Miri between the surface and 400 m height combined with Sonne ship measurements (Fuhlbrügge et al., 2016) close to the convective system.

The estimates from the simulations are calculated similarly for each of the modelled convective systems and in a manner as consistent as possible with Krysztofiak et al. (2018). For $[X]_{UTconv}$ and $[X]_{UTnoconv}$, a box of $1^\circ \times 1^\circ$ and 11-13 km altitude is selected around the convective system and $[X]_{UTconv}$ are selected where cloud ice is present. We use two different ice concentration thresholds to define both the air masses within the anvil cloud and those outside of it: a cut-off of 0.01 g kg^{-1} to define air masses within the cloud, and 0.005 g kg^{-1} to define those outside of it that are part of the simulated upper tropospheric background. We use two thresholds to define these separate air masses to ensure we derive an adequate separation between the two; air masses lying between the lower and upper cut-off show mixing and dilution of the convective outflow and neither represent background or convective outflow concentrations in a clear way. To demonstrate the sensitivity of our results to this choice, we perform a sensitivity test with two different single ice concentration thresholds to define air inside or outside the convective cloud: 0.01 g kg^{-1} and 0.005 g kg^{-1} . These results are presented in the supplement S4. For $[X]_{BL}$, a box of $0.5^\circ \times 0.5^\circ$ and 0-400 m altitude is selected around the area where the initial convective cell starts its development. For each system, two model outputs one hour apart were selected during the main phase of the outflow development for $[X]_{UTnoconv}$ and $[X]_{UTconv}$, and at the times when the initial convective cell starts developing for $[X]_{BL}$. The times and boxes chosen are given in Table A1.

Table A1: Times and latitude/longitude boxes used to calculate $[X]_{BL}$, $[X]_{UT}$ and $[X]_{UTconv}$ on November 19, 2011.

	$[X]_{BL}$ time	$[X]_{BL}$ box	$[X]_{UTnoconv}/[X]_{UTconv}$ time	$[X]_{UTnoconv}/[X]_{UTconv}$ box
Mod_Conv_4.35 N	4 UTC	4.2°N - 4.7°N 114.0°E - 114.5°E	6 UTC 7 UTC	4.1 - 5.1°N 113.3°E - 114.3°E
	5 UTC	4.2°N - 4.7°N 114.0°E - 114.5°E		4.3°N - 5.3°N 113.0°E - 114.0°E
Mod_Conv_3.75 N	7 UTC	3.35°N - 3.85°N 113.55°E - 114.05°E	9 UTC 10 UTC	3.25°N - 4.25°N 113.1°E - 114.1°E
	8 UTC	3.35°N - 3.85°N 113.55°E - 114.05°E		3.25°N - 4.25°N 112.9°E - 113.9°E
Mod_Conv_5.4N	7 UTC	5.1°N - 5.6°N 115.8°E - 116.3°E	9 UTC	5.3°N - 6.3°N 115.3°E - 116.3°E
	8 UTC	5.1°N - 5.6°N 115.8°E - 116.3°E	10 UTC	5.0°N - 6.0°N 114.9°E - 115.9°E

S3. Explanation of how error propagation to calculate f

The errors on f are calculated by propagating the standard deviations on $[X]_{UTconv}$, $[X]_{BL}$, and $[X]_{UTnoconv}$ through the arithmetic equation used to calculate f . This involves the rearrangement of equation (1) from:

$$[X]_{UTconv} = f \cdot [X]_{BL} + (1 - f) \cdot [X]_{UTnoconv} \quad (1)$$

to:

$$f = ([X]_{UTconv} - [X]_{UTnoconv}) / ([X]_{BL} - [X]_{UTnoconv}) \quad (2)$$

The error is propagated stepwise through equation (2). First, the error is propagated through the subtraction arithmetic via

$$\gamma = \sqrt{(\alpha^2 + \beta^2)} \quad (3)$$

Where x and y are variables, z is the sum or difference of both variables, and the associated errors on each variable are α , β , and γ , respectively, as $x \pm \alpha$, $y \pm \beta$, and $z \pm \gamma$. In the next step, the errors are propagated through the division operation in equation (2). The errors on f (expressed as $f \pm \varepsilon$) are calculated by using the errors on the numerator and denominator (expressed from now on as γ and γ' , respectively) calculated by equation (3) within the following equation:

$$\varepsilon = f \times \sqrt{\left(\frac{\gamma}{x-y}\right)^2 + \left(\frac{\gamma'}{x'-y'}\right)^2} \quad (4)$$

where f is the fraction calculated in equation 2, and the two terms within the square root refer to the numerator and denominator. Thus, x , y , x' , and y' would refer to $[X]_{UTconv}$, $[X]_{UTnoconv}$, $[X]_{BL}$, and $[X]_{UTnoconv}$, respectively.

S4. Sensitivity Analysis of Choice of Threshold in Ice Concentration

We test the sensitivity of the simulated mean bromoform concentrations in the convective and non-convective UT to the choice of ice concentration threshold. We also test the impact that this has on the calculations of the fraction f . Here we test two ice concentrations: 0.01 g/kg and 0.005 g/kg and the results from both tests are shown in Table S2.1 and S2.2, respectively.

Table S2.1: Estimates from the model simulations of the CHBr_3 concentrations in the UT outside convection $[\text{X}]_{\text{UTnoconv}}$ and in the UT within convection $[\text{X}]_{\text{UTconv}}$ calculated using an ice concentration threshold of 0.01 g/kg to delineate cloud and cloud free. f is the air fraction originating from the boundary layer and transported by convection. Details on the method used are given in Appendix A.

	$[\text{X}]_{\text{UTnoconv}}$ (mean $\pm 1\sigma$)	$[\text{X}]_{\text{UTconv}}$ (mean $\pm 1\sigma$)	fraction f
Mod_Conv1	0.34 ± 0.15	0.62 ± 0.18	0.16 ± 0.13
Mod_Conv2	0.41 ± 0.18	0.62 ± 0.13	0.26 ± 0.30
Mod_Conv3	0.36 ± 0.13	0.56 ± 0.12	0.17 ± 0.15

Table S2.2: Estimates from the model simulations of the CHBr_3 concentrations in the UT outside convection $[\text{X}]_{\text{UTnoconv}}$ and in the UT within convection $[\text{X}]_{\text{UTconv}}$ calculated using an ice concentration threshold of 0.005 g/kg to delineate cloud and cloud free. f is the air fraction originating from the boundary layer and transported by convection. Details on the method used are given in Appendix A.

	$[\text{X}]_{\text{UTnoconv}}$ (mean $\pm 1\sigma$)	$[\text{X}]_{\text{UTconv}}$ (mean $\pm 1\sigma$)	fraction f
Mod_Conv1	0.29 ± 0.07	0.58 ± 0.20	0.16 ± 0.11
Mod_Conv2	0.33 ± 0.13	0.61 ± 0.13	0.32 ± 0.24
Mod_Conv3	0.34 ± 0.11	0.56 ± 0.11	0.18 ± 0.14